Normal metal - insulator - superconductor thermometers and coolers with titanium-gold bilayer as the normal metal

IOP Conf. Series: Journal of Physics: Conf. Series **969** (2018) 012090 doi:10.1088/1742-6596/969/1/012090

Normal metal - insulator - superconductor thermometers and coolers with titanium-gold bilayer as the normal metal

I M W Räisänen, Z Geng, K M Kinnunen and I J Maasilta

Nanoscience Center, Department of Physics, University of Jyväskylä, P.O. Box 35 (YFL), FI-40014 University of Jyväskylä, Finland

E-mail: ilmo.raisanen@jyu.fi

Abstract. We have fabricated superconductor - insulator - normal metal - insulator - superconductor (SINIS) tunnel junctions in which Al acts as the superconductor, AlOx is the insulator, and the normal metal consists of a thin Ti layer (5 nm) covered with a thicker Au layer (40 nm). We have characterized the junctions by measuring their current-voltage curves between 60 mK and 750 mK. For comparison, the same measurements have been performed for a SINIS junction pair whose normal metal is Cu. The Ti-Au bilayer decreases the SINIS tunneling resistance by an order of magnitude compared to junctions where Cu is used as normal metal, made with the same oxidation parameters. The Ti-Au devices are much more robust against chemical attacks, and their lower tunneling resistance makes them more robust against static charge. More significantly, they exhibit significantly stronger electron cooling than Cu devices with identical fabrication steps, when biased close to the energy gap of the superconducting Al. By using a self-consistent thermal model, we can fit the current-voltage characteristics well, and show an electron cooling from 200 mK to 110 mK, with a non-optimized device.

1. Introduction

Normal metal - insulator - superconductor (NIS) tunnel junctions are versatile and useful devices for thermometry, cooling, and metrological applications for the definition of the ampere [1, 2, 3]. In most applications, the normal metal lead needs to be highly conductive, so copper has been a common choice. However, Cu has its problems when the junctions have to go through additional fabrication steps, such as a second layer of resist coating, plasma etching etc. We have observed that the Cu electrode degrades strongly with heating, and in contact with many commonly used solvents in electron beam resists. The Cu lead can degrade even in the lift-off step, if acetone is used as the lift-off solvent and if it has absorbed some moisture, e.g., from air. With such conditions acetic acid is generated, which can etch some of the Cu [4]. This degradation effect is demonstrated in Figure 1a, where nanopores are visible in an NIS sample with a Cu normal metal electrode. Thus, it is desirable to find other alternatives for the normal metal.

The Cu lead can be replaced with Au. However, Au has a well known adhesion problem with the commonly used oxidized or nitridized Si substrates. In order to overcome this issue, a thin wetting layer of Cr or Ti underneath the Au layer is typically used. Here, we implement a thin Ti layer (5 nm) underneath a thicker Au layer (40 nm) in the normal metal fabrication, similar to Refs. [5, 6]. Even though Ti is a superconductor below 0.5 K [7], with such a large mismatch

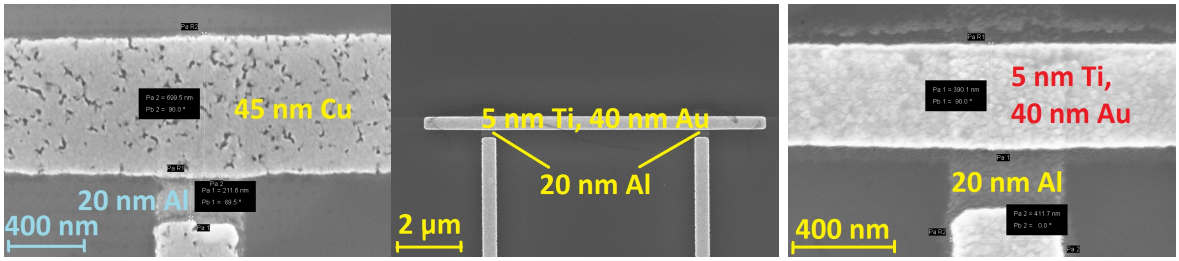

(a) (b) (c)

Figure 1: Scanning electron micrographs of (a) an NIS junction whose normal metal is Cu with clear degradation of Cu, (b) a SINIS junction pair whose normal metal is a Ti-Au bilayer, and (c) an NIS junction whose normal metal is Ti-Au.

of the layer thicknesses the direct contact with the Au layer causes the whole bilayer to be in normal state due to the inverse proximity effect [8].

In this article, we present the fabrication and measurement of SINIS tunnel junction pairs in which the superconductor is Al, the insulator is AlOx and the normal metal is a Ti-Au bilayer, see Figure 1b. The junctions are fabricated on a nitridized Si substrate using electron beam lithography, electron beam evaporation of the Al, Ti and Au films (thicknesses 20 nm, 5 nm and 40 nm, respectively), and in-situ oxidation of the Al in $\sim$ 40 mbar of pure oxygen for 4 min to form the tunnel barrier. As can be seen in Figure 1c, the Ti-Au island is smooth and uniform, and it never exhibited any obvious degradation after the lift-off in contrast to some Cu island samples (Figure 1a). We compare the current-voltage characteristics and cooling effects between 60 mK and 750 mK to otherwise identically fabricated SINIS junctions, but whose normal metal is Cu instead of Ti-Au. We found that the total tunneling resistances of the Ti-Au bilayer SINIS junctions were around 2.3 kΩ immediately after lift-off, and the resistances decreased by $\sim$ 10 % when the junctions were 6 weeks in normal atmosphere. This behavior is in contrast with Cu based SINIS junctions, which typically have an order of magnitude higher tunneling resistance with the same oxidation parameters, and a trend of increasing tunneling resistance with age.

2. Current-voltage characteristics

The current I through a SINIS junction pair can be written in a symmetrized form as [1]

$$I(V) = \frac{1}{2eR_T}\int_{-\infty}^{\infty} N_S(E)[f_N(E-eV) - f_N(E+eV)]dE, \tag{1}$$

where V is the total voltage, R_T is the total tunneling resistance of the SINIS junction pair, and $f_N(E)$ denotes the Fermi-Dirac distribution in the normal metal lead at energy E. The quantity N_S is the density of states (DOS) in the superconductor and it is typically given by

$$N_S(\epsilon, T_S) = \left|\mathrm{Re}\left(\frac{\epsilon + i\Gamma}{\sqrt{(\epsilon+i\Gamma)^2 - \Delta^2(T_S)}}\right)\right|, \tag{2}$$

where ϵ is the energy and T_S is the temperature of the superconductor. The quantity Δ is the energy gap of the superconductor. The temperature dependence of $\Delta(T_S)$ can be calculated based on the BCS theory. Finally, Γ denotes the Dynes parameter [9, 10], which is used to describe the broadening of the effective DOS, leading to sub-gap current through the junctions at voltages lower than Δ/e. Below $T_S < 0.4\ T_C$ the gap has a very weak temperature dependence, in which case a SINIS device is sensitive to the normal metal electron temperature alone through $f_N(E)$.

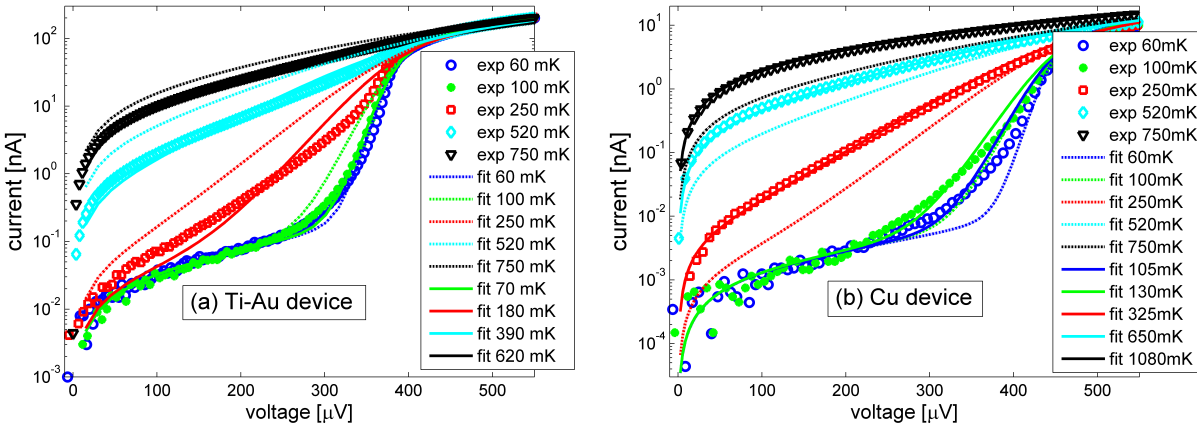

Figure 2: Measured current-voltage characteristics (open symbols). Theory fits of Equations (1) and (2) when assuming electron temperature to equal the cryostat temperature (dashed lines) and when electron temperature is used as a fit parameter (solid lines).

We measured the current-voltage characteristics of Ti-Au and Cu SINIS devices at five different temperatures between 60 mK and 750 mK. In Figure 2 we present the data in log-linear scale, together with equilibrium model ($T_S = T_N$) theory based on Equations (1) and (2). Figure 2a shows the data for the Ti-Au device, while Figure 2b presents the data for the Cu device. First, we make the theory fitting by assuming that the electron temperature in the normal metal equals the cryostat temperature, measured with a separate RuOx thermometer at the sample stage. These fits are shown by dashed lines. The quantities Γ and Δ, on the other hand, were used as fitting parameters. The fits give estimates $\Gamma = 6.5 \times 10^{-4} \times \Delta$ and $\Gamma = 3.5 \times 10^{-4} \times \Delta$ for the Ti-Au device and the Cu device, respectively, whereas for Δ, we obtain $\Delta = 188$ μeV for the Ti-Au device and $\Delta = 220$ μeV for the Cu device. From Figure 2 we see that for higher bath temperatures, the fits shown by dashed lines are not good. Nevertheless, from the lowest 60 mK data, Γ and Δ can be determined quite accurately. The differences in Γ and Δ between the two devices are interesting. The variation of Γ is perhaps not surprising, considering that the total tunneling resistance R_T, determined from the slope of the $I-V$ curves in a large bias regime (-7 mV ... +7 mV), varies by an order of magnitude between the two samples, 2.1 kΩ for the Ti-Au device and 28 kΩ for the Cu device. This can lead to different amount of absorbed noise power leading to variation of Γ due to photon assisted tunneling [10]. The variation of Δ, on the other hand, is an indication of differences in Al quality, a bit surprising result as the same evaporator and the same Al thickness were used.

The fits shown by dashed lines in Figure 2, where we assumed the electron temperature to equal the cryostat temperature, are not satisfactory, especially at temperatures above 100 mK. Therefore, we take the electron temperature as another fit parameter, see the solid lines in Figure 2. For the Ti-Au device, we see that the theoretical $I-V$ curves match the measurement data fairly well when the electron temperature is lowered from the measured bath temperature value. However, for the case of the Cu device, the electron temperature needs to be made higher than the bath temperature for the simulations to match the experimental data. Most notably, though, the fits are still not good at the lowest temperatures for both junctions types, most clearly seen for the Ti-Au device at bath temperature 250 mK.

3. Thermal model and cooling of electrons in the normal metal

To fully understand the measured $I-V$ curves, we must consider the cooling effect of an NIS junction. It is based on the fact that only electrons from the normal metal that have at least energy Δ can enter the superconductor. Since electrons of the normal metal obey the Fermi-Dirac distribution, there are hot electrons which can tunnel to the superconductor also at bias voltages $eV < \Delta$. Since only hot electrons escape from the normal metal, the temperature of remaining electrons in the normal metal lead decreases. The bias dependent heat flow from the normal metal to the superconductor in a single NIS junction is [1]

$$\dot{Q}_{\mathrm{cool}} = \frac{1}{e^2 R_T}\int_{-\infty}^{\infty}(E-eV)n_S(E)[f_N(E-eV)-f_S(E)]dE, \tag{3}$$

where $n_S(E)$ and $f_S(E)$ are the density of states and the Fermi-Dirac distribution in the superconductor at energy E, respectively. In dynamic equilibrium, cooling by the junctions in a SINIS device is balanced by the inflow of heat from the surroundings. This leads to the equation for a symmetric SINIS cooler [11]

$$2\dot{Q}_{\mathrm{cool}} = A(T_{\mathrm{bath}}^5 - T_N^5) + \beta(2\dot{Q}_{\mathrm{cool}} + IV) + I^2 R_N, \tag{4}$$

which describes three heating mechanisms: The first term on the right represents the heating from the substrate phonons that are at temperature T_{bath}. The substrate phonons couple to the normal metal electrons that are at temperature T_N. The symbol A denotes the coupling strength constant and it is given by $A = \Sigma\Omega$, where Σ is the electron-phonon coupling constant and Ω is the volume of the normal metal lead. The second term on the right describes the flow of heat from the superconductor to the normal metal via phonons or back-tunneling, where $(0 \leq \beta \leq 1)$ is the fraction of total heat deposited in the superconductor that flows back to the normal metal. The third term on the right is the Joule heating of the normal metal whose resistance is R_N.

In Figure 3, we fit the $I-V$ curves with Equation (1), but including self-consistently the thermal model described by Equations (3) and (4) to the experimental data, using A, $T_S = T_{\mathrm{bath}}$, β and R_N as fitting parameters. For the Ti-Au device, the best fit is obtained for each bath temperature with $A = 5.78 \times 10^{-10}$ W/K^5, $\beta = 0.05$, and $R_N = 50\ \Omega$. On the other hand, for the Cu device, we get $A = 3.18 \times 10^{-10}$ W/K^5, $\beta = 0.05$, and $R_N = 40\ \Omega$. The fit quality improves significantly compared to those of the equilibrium model (Figure 2), specifically, the thermal model can account for the bias dependent curvature of the $I-V$ curves. The volume of the normal metal lead was measured with an atomic force microscope (AFM) and a scanning electron microscope (SEM), and it is 0.18 μm^3 for both junction types. We thus get estimates for the electron-phonon coupling constants, giving us for the Ti-Au bilayer $\Sigma_{\mathrm{Ti\text{-}Au}} = (4.2 \pm 0.3) \times 10^9$ W/(K^{5}m^3), and for Cu $\Sigma_{\mathrm{Cu}} = (2.3 \pm 0.3) \times 10^9$ W/(K^{5}m^3). These values can be compared with literature values for Cu, Au and Ti thin films, with $\Sigma_{\mathrm{Cu}} = 2 \times 10^9$ W/(K^{5}m^3) [12, 13], $\Sigma_{\mathrm{Au}} = 2.4 \times 10^9$ W/(K^{5}m^3) [14] and $\Sigma_{\mathrm{Ti}} = 1.3 \times 10^9$ W/(K^{5}m^3) [15], respectively.

In Figure 4 we plot the bias dependent electron temperature T_e of the normal metal obtained from the thermal model fits. We see that the electron temperature in the Ti-Au island (Figure 4a) decreases from 200 mK to 110 mK when the bias voltage is around 350 μV, with weaker effect at higher temperatures as expected. However, the Cu island clearly cools much less (Figure 4b). The main reason for the weaker cooling effect is the higher tunneling resistance (28 kΩ) in the Cu device than in the Ti-Au device (2.1 kΩ), implying a higher and/or wider tunneling barrier. However, cooling of the normal metal electrodes could be possibly made significantly stronger by increasing the junction area which is now only (0.13 ± 0.01) μm^2. The fact that the 60 mK and 100 mK bath temperature curves merge quickly after zero bias for the Ti-Au case in Figure 4a explains the similarity of the measured $I-V$ curves at 60 mK and 100 mK shown in Figure 3a.

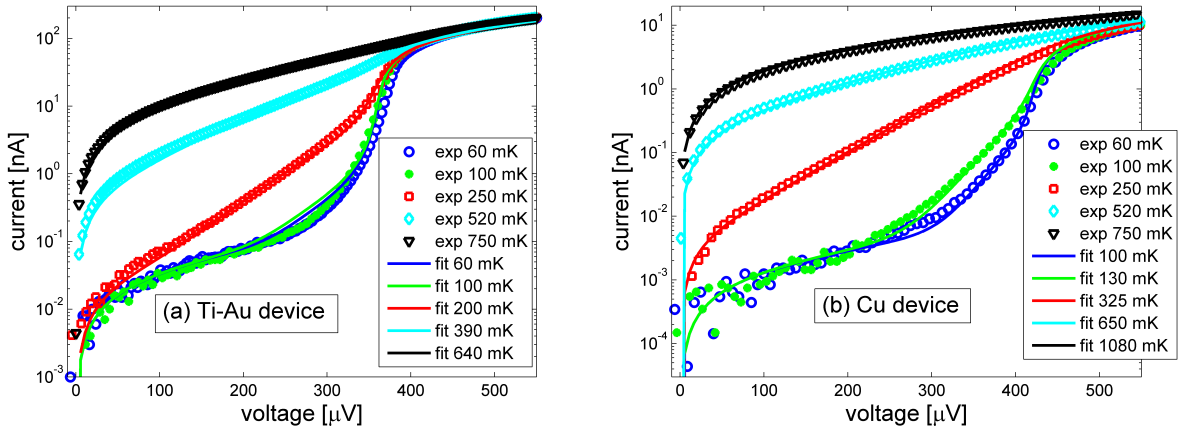

Figure 3: Measured current-voltage characteristics (open symbols) with thermal model fits using Equations (3) and (4) (solid lines).

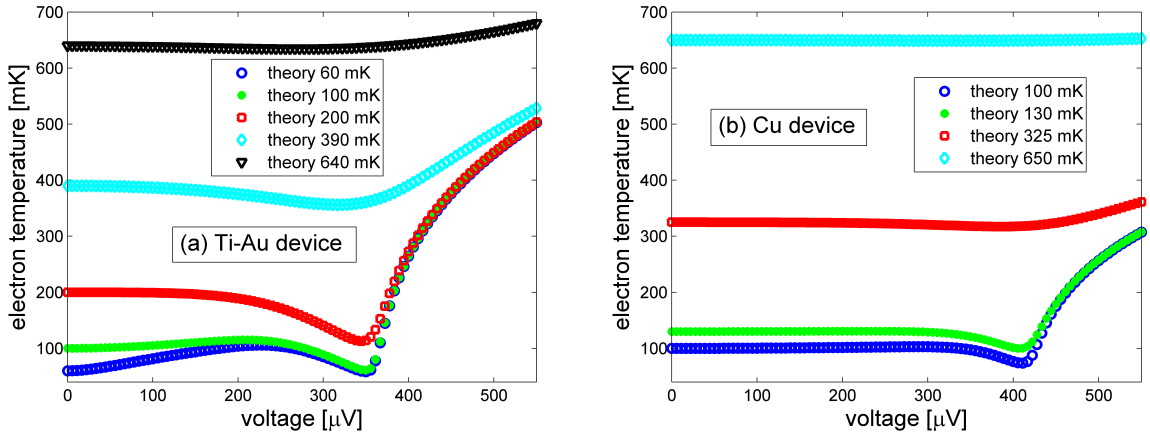

Figure 4: Electron temperature of the normal metal lead with respect to DC voltage bias obtained from the thermal model fits shown in Figure 3.

Figure 5 presents the cooling power $2\dot{Q}_{\mathrm{cool}}$ by the tunnel junctions and the corresponding coefficient of performance $\mathrm{COP} = 2\dot{Q}_{\mathrm{cool}}/(IV)$ of the Ti-Au and Cu cooler devices. The Ti-Au device has an order of magnitude higher cooling power than the Cu device as expected, and the cooling power is highest at highest temperatures for both devices. Around the optimal bias voltage for cooling, the cooling power and the COP match well with literature values $\dot{Q}_{\mathrm{cool}} = 0.06\Delta^2/(e^2 R_T)$ and $\mathrm{COP} = 0.25$ at $T = 0.25\Delta/k_B$ [1].

As the current-voltage characteristics of an NIS junction depend only on the temperature of the normal metal electrode when T_S is well below T_C, which can be seen in Equation (1), a measurement of voltage V at a constant current also gives the normal metal electron temperature in quasiequilibrium conditions [1]. We have also measured voltage vs. cryostat temperature curves to confirm that the Ti-Au junctions can also be operated in such a manner.

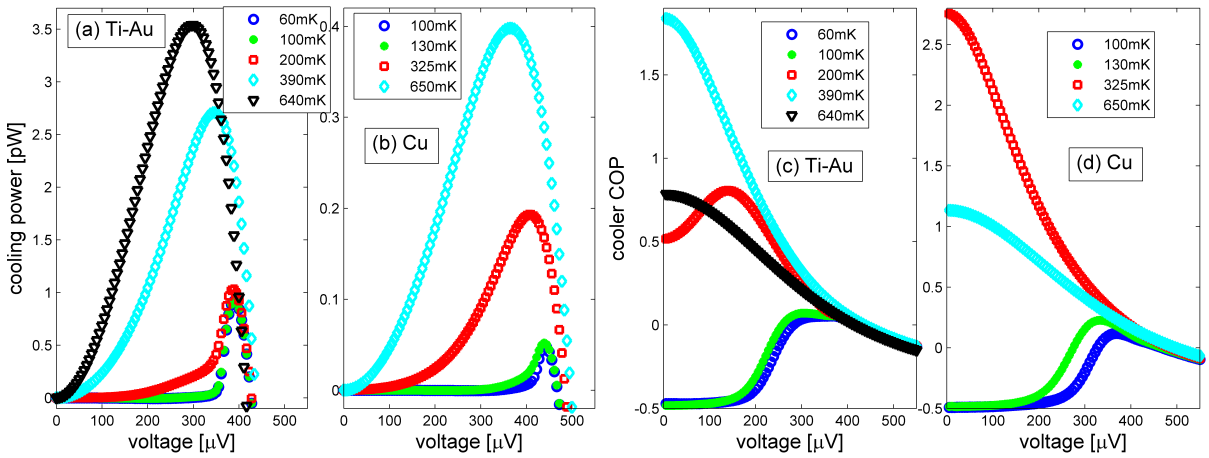

Figure 5: Cooling power and coefficient of performance of the Ti-Au and Cu cooler devices obtained from the thermal model fits shown in Figure 3.

4. Summary

This work shows that a Ti-Au bilayer is a promising material for the normal metal electrode in NIS junctions. The Ti-Au bilayer significantly improves the tolerance of the normal metal to solvents and thus further processing rounds, as compared to Cu. With the same processing parameters as with Cu devices, the tunneling resistance of Ti-Au devices is reduced by an order of magnitude, which, as we demonstrated, improves the electron cooling effect.

We managed to fit the experimental $I-V$ characteristics only with the help of a thermal model that took into account bias dependent cooling and heating of the NIS junctions, demonstrating a strong cooling effect even in a non-optimized structure. In the future, we plan to study the effects of the Ti-Au bilayer on the microscopic barrier properties in a more detailed manner, and optimize a cooler structure to demonstrate a much stronger cooling effect.

Acknowledgments

This project is supported by Finnish Cultural Foundation and the Academy of Finland project number 298667.

References

[1] Giazotto F, Heikkilä T T, Luukanen A, Savin A M and Pekola J P 2006 *Rev. Mod. Phys* **78** 217–74
[2] Pekola J P, Saira O-P, Maisi V F, Kemppinen A, Möttönen M, Pashkin Yu A and Averin D V 2013 *Rev. Mod. Phys.* **85** 1421–72
[3] Muhonen J T, Meschke M and Pekola J P 2012 *Rep. Prog. Phys.* **75** 046501
[4] Kagwade S V, Clayton C R, Chidambaram D and Halada G P 2001 *Electrochimica Acta* **46** 2337–42
[5] Koppinen P J, Isotalo T J and Maasilta I J 2009 *AIP Conf. Proc.* **1185** 318
[6] Faivre T, Golubev D S and Pekola J P 2015 *Appl. Phys. Lett.* **106** 182602
[7] Falge R L Jr 1963 *Phys. Rev. Lett.* **11** 248–50
[8] Fominov Ya V and Feigel'man M V 2001 *Phys. Rev.* B **63** 094518
[9] Dynes R C, Garno J P, Hertel G B and Orlando T P 1984 *Phys. Rev. Lett.* **53** 2437–40
[10] Pekola J P, Maisi V F, Kafanov S, Chekurov N, Kemppinen A, Pashkin Yu A, Saira O-P, Möttönen M and Tsai J S 2010 *Phys. Rev. Lett.* **105** 026803
[11] Chaudhuri S and Maasilta I J 2012 *Phys. Rev.* B **85** 014519
[12] Roukes M L, Freeman M R, Germain R S, Richardson R C and Ketchen M B 1985 *Phys. Rev. Lett.* **55** 422–5
[13] Karvonen J T, Taskinen L J and Maasilta I J 2007 *J. Low Temp. Phys.* **146** 213–26
[14] Echternach P M, Thoman M R, Gould C M and Bozler H M 1992 *Phys. Rev.* B **46** 10339–44
[15] Manninen A J, Suoknuuti J K, Leivo M M and Pekola J P 1999 *Appl. Phys. Lett.* **74** 3020–22